Limnol. Oceanogr., 27(3), 1982, 500–509

Bio-optical classification and model of natural waters. 2[1]

Karen S. Baker and Raymond C. Smith[2]
Scripps Institution of Oceanography A-030, University of California,
San Diego, La Jolla 92093

Abstract

A bio-optical technique is presented which allows both the classification and optical modeling of natural waters. The spectral diffuse attenuation coefficient for irradiance (300–700 nm) has been related to two biological quantities: the total concentration of chlorophyll-like pigments and the dissolved organic material (DOM). The model is a component model which augments our previous work in that it includes new data in the analysis, utilizes an improved analytic fit, extends into the UV region of the spectrum, and adds a DOM component. Our model, which permits quantitative calculation of spectral irradiance at any point in the water column in a variety of nonterrigenous water types, facilitates predictive modeling.

The term bio-optical state was coined (Smith and Baker 1978*a*) to represent a measure of the total effect of biological material on the optical properties of natural waters. We then introduced (Smith and Baker 1978*b*) a general technique for optically classifying and predictively modeling natural waters in terms of the total chlorophyll-like pigment concentration in these waters, hereafter referred to as SB1. The method was built upon two concepts: the pioneering insight of Jerlov (1951, 1976) that ocean waters could be optically classified; and the idea that the diffuse attenuation coefficient for irradiance could be partitioned (Riley 1956; Steele and Menzel 1962; Yentsch 1963) into the components responsible for the total attenuation (e.g. water, phytoplankton, and other attenuating substances). Our first classification (SB1) was based on spectral irradiance data from a wide range of ocean waters varying in chlorophyll concentrations from 0.01 to 10 mg Chl $a \cdot m^{-3}$ (Tyler and Smith 1967, 1970; Smith and Tyler 1968; Smith 1973; Smith and Baker 1978*a*,*b*) whose dissolved and suspended materials are primarily of biogenous origin. We here present an amended version of our classification model which includes new data, uses an improved analytic fit, extends into the UV region down to 300 nm, revises the 600–700-nm region where the model was least accurate, and quantitatively includes attenuation due to dissolved organic material.

The rationale for choosing the total diffuse attenuation coefficient for irradiance, $K_T(\lambda)$, to characterize the bio-optical state of ocean water, has been discussed elsewhere (Smith and Baker 1978*a*). Our primary reason continues to be that K_T is the optical property which relates irradiance just beneath the ocean surface, $E(0^-,\lambda)$, to irradiance at depth, $E(z,\lambda)$:

$$E(z,\lambda) = E(0^-,\lambda)\exp[-\int K_T(\lambda,z)\cdot dz], \quad (1)$$

and it is this quantity which is of direct interest in the study of aquatic photoprocesses. Thus K_T is both the property that is directly derivable from spectral irradiance measurements and the property, when known, that allows the spectral irradiance at depth to be calculated from a knowledge of $E(0^-,\lambda)$. In our view the simplicity of dealing directly with K_T, for both measurement and application, rather than the dual conversion to an inherent optical property such as the absorption coefficient and back again, outweighs the disadvantages of its apparent optical property status. This is especially true since the "quasi-inherent" characteris-

[1] This research was supported by NASA grant NSG 1641 and U.S. EPA grants R 806 489-02 and R 806 372-02. This study is also a contribution to the research encouraged by the IAPSO Working Group on Optical Oceanography.

[2] Present address: Department of Geography, Univ. Calif., Santa Barbara 93106.

Table 1. Cruises that provided data for present model.

Cruise		Location	No. of stations
Fresnel I	28 Nov–13 Dec 68	Gulf of California	6
Fresnel II	16 Mar–31 Mar 71	Gulf of California	5
Researcher	12 Oct–30 Oct 77	Gulf of Mexico	9
Gyre	8 Nov–20 Nov 78	Gulf of Mexico	7
Knorr	20 Jul–15 Aug 78	South Pacific	11
New Horizon	24 Feb–11 Mar 79	North Pacific U.S. Coast	6
Oceanus	18 Aug–29 Aug 79	North Atlantic U.S. Coast	10

tics of $K_T(z,\lambda)$ have been demonstrated (Højerslev 1974; Baker and Smith 1979).

Data and methods

Downwelling spectral irradiances have been measured as a function of depth with the submersible Scripps spectroradiometer described in detail elsewhere (Tyler and Smith 1966, 1970). New data have been obtained with the UV submersible spectroradiometer (Smith et al. 1979) designed especially to include the MUV region from 280 to 340 nm in addition to the visible region. From these measurements the spectral diffuse attenuation coefficient can be directly determined for the water column between the depths (e.g. z_1 and z_2) of irradiance measurements by

$$K_T(\lambda) = [-1/(z_2 - z_1)]\ln[E(z_2,\lambda)/E(z_1,\lambda)]. \quad (2)$$

Alternatively, all the depth data for a single wavelength can be fit by least-squares to a straight line on a semilog plot, the slope of which gives $K_T(\lambda)$

$$K_T(\lambda) = [-1/E(z,\lambda)]\mathrm{d}[\ln E(z,\lambda)\cdot 1/\mathrm{d}z]. \quad (3)$$

The latter method has the advantage of averaging out variations in depth due to rough seas, but should also be recognized as an oversimplification since it assumes that the water column is homogeneous with depth and ignores effects caused by changes in spectral irradiance with depth. Despite these limitations, the procedure provides a good first-order estimate for K_T, especially in the waters containing very little terrigenous material (i.e. low scattering to absorption ratio) with which we are dealing here.

We have previously described the data for our analysis (Smith and Baker 1978*b*). We have now added spectral irradiance data and biological data from subsequent cruises (Table 1). Although we continue to base our analysis on all our $K_T(\lambda)$ data, we emphasize here those which include the MUV region of the spectrum. Although these data are limited, they comprise the first set to span a range of biogenous water types for the spectral region from 300 to 400 nm.

The component model presented here, based on the idea that K_T can be partitioned into components, is summarized by

$$K_T(\lambda) = K_W(\lambda) + K_C(\lambda) + K_D(\lambda) \quad (4)$$

(Table 2). The clear water component, $K_W(\lambda)$, is known and based on an accurate and consistent set of data (Smith and Baker 1981). The chlorophyll component, $K_C(\lambda)$, accounts for all "chlorophyll-like" pigments that covary with chlorophyll. The dissolved organic material component, $K_D(\lambda)$, accounts for the remaining absorption, as discussed below. It is clear from this equation, which contains no explicit term for suspended matter, that this representation models biogenous but nonterrigenous waters.

Chlorophyll component

To compare waters of various chlorophyll concentrations consistently, we define

$$C_K = (1/K_{\mathrm{PAR}}) \int_0^{K_{\mathrm{PAR}}^{-1}} C(z)\cdot \mathrm{d}z \quad (5)$$

where C_K is the average chlorophyll concentration in the water column to a depth of one attenuation length K_{PAR}^{-1} and $C(z)$ is the chlorophyll concentration (mg

Table 2. Equations of bio-optical classification and model. Spectral constants $K_W(\lambda)$ (m^{-1}), $k_c(\lambda)$ and $k_c'(\lambda)$ [$m^{-1} \cdot (mg\ Chl \cdot m^{-3})^{-1}$] given in Table 3. Values of C_0 = 0.50 mg Chl·m^{-3} and of λ_0 = 380 nm are constants. Højerslev (1980) values (Table 4) of k_d = 0.565 $m^{-1} \cdot (mg\ DOM \cdot liter^{-1})^{-1}$ and k_d' = 0.014 nm^{-1} are assumed for this work.

$$K_T(\lambda) = K_W(\lambda) + K_C(\lambda) + K_D(\lambda)$$
$$K_C(\lambda) = k_c(\lambda) \cdot C_K \cdot \exp[-k_c'^2(\lambda) \cdot (\log C_K - \log C_0)^2] + 0.001 C_K^2$$
$$K_D(\lambda) = k_d(\lambda_0) \cdot D \cdot \exp[-k_d'(\lambda - \lambda_0)]$$

Input: C (mg Chl·m^{-3}) and D (mg DOM·liter^{-1})

Output: $K_T(\lambda)$ (m^{-1})

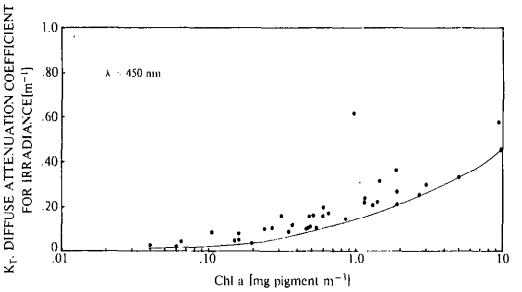

Fig. 1. Diffuse attenuation coefficient for wavelength 450 nm vs. chlorophyll concentration, where we use chlorophyll to refer to all chlorophyll-like pigments. Solid line for minimum envelope represents K_T data for which attenuation due to DOM is postulated to be negligible.

Chl·m^{-3}) at depth z (m). K_{PAR} is the total attenuation coefficient for photosynthetically available radiant energy (PAR), i.e. that attenuation coefficient determined by a quantum meter with a constant response between 350 and 700 nm (Jerlov and Nygård 1969; Tyler 1975; Booth 1976). The chlorophyll concentration at each depth is determined fluorometrically after extraction in 90% acetone (Strickland and Parsons 1968; Smith et al. 1981).

Figure 1 is an example of the data where the diffuse attenuation coefficient, K_T (450 nm), has been plotted vs. chlorophyll concentration, C_K. If we follow the suggestion of Tyler (1975) and our previous argument with respect to nonlinear biological effects (Smith and Baker 1978*b*), these data indicate that there is a minimum envelope represented by the solid line in Fig. 1. We suggest that this minimum envelope represents $K_T(\lambda)$ data for which the attenuation due to DOM is negligible compared to that due to viable phytoplankton, for which we are using C_K as a measure. $K_T(\lambda)$ values above the minimum envelope can be expected to have significant attenuation due to DOM.

In Fig. 2 are presented representative full spectral $K_T(\lambda)$ curves (solid lines) for those data where we believe the influence of DOM to be negligible. Significant features of these data, which are the first continuous $K_T(\lambda)$ data to span the spectral region from 300 to 700 nm, include: increased strong attenuation with decreasing wavelength in the 300–400-nm region; a broad attenuation "bump" centered about 430 nm; an attenuation minimum that moves from about 450 to 560 nm with increasing chlorophyll concentration; a sharp increase in attenuation, due to the absorption of pure water, in the spectral regions between 500–600 nm and 700–740 nm; a broad region between 640 and 700 nm where the $K_T(\lambda)$ data sometimes cross, becoming lower for increasing C_K concentrations.

The first observation, that there is increased attenuation of biogenic material directly related to its chlorophyll concentration, is consistent with Yentsch's observation (Yentsch 1962, 1979; Yentsch and Reichert 1962) that all the light absorbed at short wavelengths is not active in the photochemistry of photosynthesis. This absorption, which increases with wavelengths shorter than 400 nm, is directly associated with viable phytoplankton (for which we used C_K as a measure), can be observed within the absorption of phytoplankton samples directly measured in laboratory spectrophotometers (Shibata 1958), and should be distinguished from absorption of dissolved organic material, which looks similar. This emphasizes the desirability of carefully distinguishing among the various biogenic components that compete for underwater radiant energy.

The second observation, the broad chlorophyll-like bump near 430 nm, is consistent with laboratory measurements

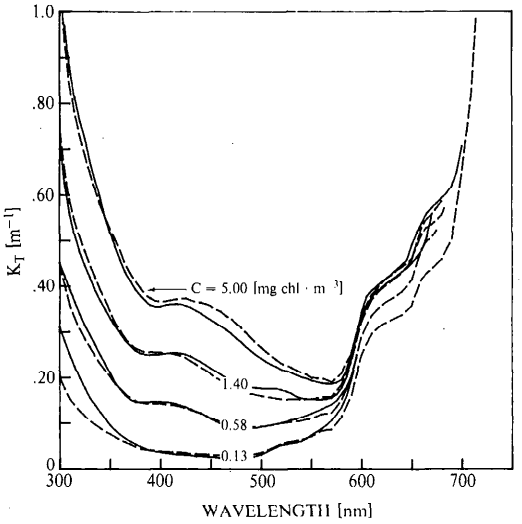

Fig. 2. Spectral diffuse attenuation coefficient vs. wavelength. Solid lines represent field measurements where influence of DOM is negligible. Broken lines represent calculated values of $K_T(\lambda)$ using Eq. 6.

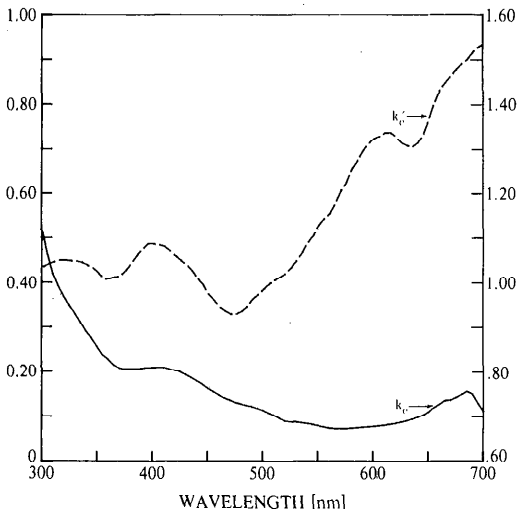

Fig. 3. Chlorophyll component spectral fit parameters vs. wavelength. Solid line (left axis) represents $k_c(\lambda)$ of Eq. 6; broken line (right axis) represents exponential term $k_c'(\lambda)$ of Eq. 6.

of marine phytoplankton (Duntley et al. 1974; Kiefer et al. 1979) and in situ determinations of the specific spectral absorption of phytoplankton (Smith and Baker 1978*b*; Morel and Prieur 1977). The third observation, relating the wavelength of maximum transmittance to C_K, has been discussed in detail by Morel and Smith (1974). The fourth observation, indicating the impact of the absorption of pure water on $K_T(\lambda)$, is widely known.

The last observation with respect to the $K_T(\lambda)$ data in Fig. 2, that "anomalous" results may occur in the 640–700-nm region, has been noted in earlier data (Tyler and Smith 1970; Morel and Prieur 1975) and theoretically explained (Gordon 1979) and modeled (Preisendorfer 1979) as being due to in vivo fluorescence of Chl *a*. In this regard it should be noted that Eq. 1–3 apply strictly to a source-free medium. Even the derivation of the absorption coefficient by means of the usual Gershun-Preisendorfer relations (Preisendorfer 1976) assumes no fluorescence as a first approximation. However, the in vivo fluorescence of chlorophyll *a* does introduce an error into our model, especially in the 650–700-nm region. We are currently investigating how best to accommodate in vivo fluorescence in a predictive model. For many purposes this is an insignificant source of error.

It is possible to analyze the $K_T(\lambda)$ data with negligible DOM (i.e. those points on the minimum envelope) to obtain the chlorophyll component for the present classification scheme. This is similar to our previous technique of analysis (Smith and Baker 1978*b*). Improvements on our earlier work include: an enlarged data base; data down to 300 nm; and a single-curve fit (*see Fig. 1*) rather than the previous two-line fit.

The equation of fit has the form [following Eq. 4 and assuming $K_D(\lambda) = 0$]:

$$\begin{aligned} K_T(\lambda) - K_W(\lambda) &= K_C(\lambda) \\ &= k_c(\lambda) \cdot C_K \\ &\quad \cdot \exp[-k_c'^2(\lambda) \\ &\quad \cdot (\log C_K - \log C_0)^2] \\ &\quad + 0.001 C_K^2. \end{aligned} \tag{6}$$

In this equation $k_c(\lambda)$, k_c', and C_0 are spectral fit parameters. The tabulated values of these parameters are given in Table 3 and plotted in Fig. 3.

Table 3. Spectral constants $K_W(\lambda)$, $k_c(\lambda)$, and $k_c'(\lambda)$ for equations in Table 2. $K_W(\lambda)$ values are for seawater, values for freshwater from Smith and Baker (1981: table 1).

nm	K_W	k_c	k_c'	nm	K_W	k_c	k_c'
300	0.154	0.520	1.036	525	0.0504	0.088	1.035
305	0.135	0.466	1.042	530	0.0519	0.087	1.050
310	0.116	0.421	1.047	535	0.0544	0.085	1.068
315	0.105	0.392	1.051	540	0.0568	0.084	1.090
320	0.0944	0.368	1.051	545	0.0608	0.082	1.106
325	0.0855	0.348	1.049	550	0.0648	0.079	1.130
330	0.0765	0.331	1.049	555	0.0683	0.076	1.144
335	0.0701	0.312	1.046	560	0.0717	0.073	1.155
340	0.0637	0.291	1.040	565	0.0762	0.072	1.176
345	0.0584	0.275	1.034	570	0.0807	0.072	1.205
350	0.0530	0.257	1.023	575	0.0949	0.072	1.225
355	0.0485	0.238	1.009	580	0.109	0.073	1.256
360	0.0439	0.228	1.010	585	0.1335	0.074	1.274
365	0.0396	0.216	1.013	590	0.158	0.076	1.295
370	0.0353	0.208	1.017	595	0.202	0.076	1.312
375	0.0310	0.205	1.028				
380	0.0267	0.205	1.044	600	0.245	0.077	1.324
385	0.0250	0.205	1.062	605	0.267	0.079	1.329
390	0.0233	0.207	1.077	610	0.290	0.080	1.337
395	0.0221	0.209	1.088	615	0.305	0.082	1.337
				620	0.310	0.084	1.329
400	0.0209	0.209	1.088	625	0.315	0.087	1.315
405	0.0203	0.209	1.084	630	0.320	0.090	1.308
410	0.0196	0.209	1.081	635	0.325	0.094	1.306
415	0.0190	0.206	1.070	640	0.330	0.098	1.315
420	0.0184	0.202	1.060	645	0.340	0.103	1.333
425	0.0178	0.199	1.050	650	0.350	0.110	1.366
430	0.0172	0.193	1.040	655	0.375	0.119	1.404
435	0.0171	0.186	1.027	660	0.400	0.127	1.433
440	0.0170	0.179	1.010	665	0.415	0.135	1.448
445	0.0169	0.172	0.995	670	0.430	0.137	1.463
450	0.0168	0.162	0.974	675	0.440	0.142	1.478
455	0.0172	0.155	0.961	680	0.450	0.149	1.491
460	0.0176	0.148	0.946	685	0.475	0.156	1.500
465	0.0176	0.141	0.938	690	0.500	0.150	1.516
470	0.0175	0.137	0.930	695	0.575	0.129	1.528
475	0.0185	0.131	0.930				
480	0.0194	0.128	0.936	700	0.650	0.111	1.538
485	0.0203	0.124	0.946	705	0.742	0.050	1.732
490	0.0212	0.121	0.963	710	0.834	0.050	1.732
495	0.0242	0.118	0.973	715	1.002	0.050	1.732
				720	1.170	0.050	1.732
500	0.0271	0.113	0.985	725	1.485	0.050	1.732
505	0.0321	0.108	0.996	730	1.800	0.050	1.732
510	0.0370	0.103	1.006	735	2.090	0.050	1.732
515	0.0430	0.096	1.013	740	2.380	0.050	1.732
520	0.0489	0.090	1.021	745	2.425	0.050	1.732

The reliability of the model using Eq. 6 and the tabulated values of the spectral parameters (Fig. 3, Table 3) can be demonstrated by comparing calculated values (using the appropriate C_K) with the actual experimental data. In Fig. 2 the solid curves give experimentally determined values of $K_T(\lambda)$ while the dashed curves give calculated values of $K_T(\lambda)$ for the appropriate pigment concentrations corresponding to these data. The agreement between the calculated and experimental curves is satisfactory and indicates that Eq. 6, along with the parameters listed in Table 2, provides a reliable method for estimating $K_T(\lambda)$ from a knowledge of C_K.

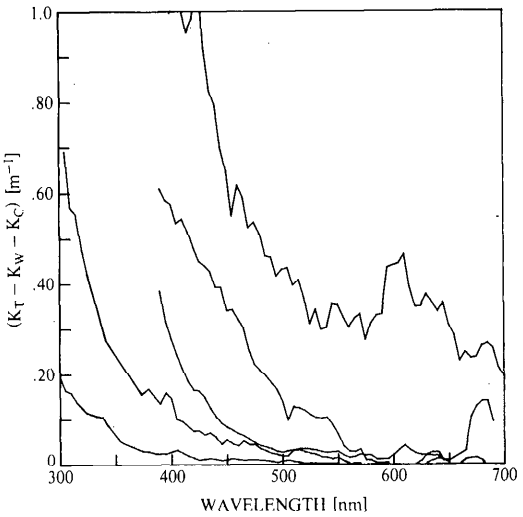

Fig. 4. Postulated attenuation due to dissolved organic material, $K_D = K_T - K_W - K_C$, vs. wavelength derived from optical field measurements of K_T.

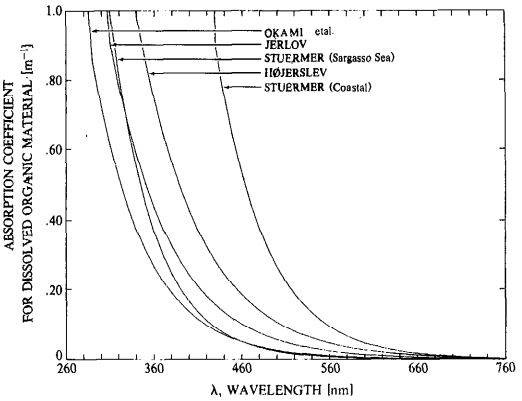

Fig. 5. Absorption vs. wavelength for investigations shown. Form of respective equations given by Eq. 9a, b and Table 4.

To improve agreement in the wavelength region above 600 nm where the fit is least accurate, we would need additional nonlinear terms in Eq. 6.

Dissolved organic material component

There is considerable evidence that absorption due to dissolved organic material (DOM, variously called yellow substance or gelbstoff or gilvin) increases exponentially with decreasing wavelength (Stuermer 1975; Jerlov 1976; Kirk 1976; Okami et al. in press; Nyquist 1979). As a consequence we expect the attenuation due to DOM to be significantly higher in the 300–375-nm region than in the visible region of the spectrum.

If, from the negligible DOM $K_T(\lambda)$-measured data, we subtract the value of $K_T(\lambda)$ as calculated, using Eq. 6 with only the chlorophyll component, we obtain curves that are generally within ±5% of zero across the spectrum, i.e. the difference between the corresponding solid and dashed curves plotted in Fig. 2, where

$$K_T(\lambda) - K_W(\lambda) - K_C(\lambda) \approx 0. \quad (7)$$

On the other hand, if we perform a similar subtraction from all the other data (corresponding to all data above the minimum envelope lines in Fig. 1), we obtain difference curves like those shown in Fig. 4, where

$$K_T(\lambda) - K_W(\lambda) - K_C(\lambda) = K_D(\lambda). \quad (8)$$

At wavelengths >500 nm most of the data agree well with the chlorophyll component model alone. In contrast, data for <500 nm show increasing attenuation with decreasing wavelength. We suggest that this difference represents the presence of varying quantities of DOM, i.e. K_D. The upper curve in Fig. 4 was included to show the effects of terrigenous scattering material in addition to dissolved organic material (as determined by ancillary data). It should be emphasized again that this model represents only biogenous water types, hence will not account for the scatter in this top curve. The addition of suspended material can significantly increase the attenuation of light.

Several recent studies (Stuermer 1975; Jerlov 1976; Takematsu et al. 1979; Nyquist 1979; Bricaud et al. 1981) provide absorption curves for DOM of the form

$$A_D(\lambda) = A_D(\lambda_0)\exp[-Y(\lambda - \lambda_0)] \quad (9a)$$

where $A_D(\lambda_0)$ (m^{-1}) is the absorption coefficient for yellow substance at the fixed

Table 4. Component constants for DOM fit to Eq. 9a, b as given by investigators who measured an absolute absorption $A_D(\lambda_0)$ (m^{-1}), including Højerslev (1980), Jerlov (1976, 1951), Okami et al. (in press), and Stuermer (1975), where Y is the exponential (Table 2: k_d') with units nm^{-1} and $A_D'(\lambda_0)$ is a specific absorption (Table 2: k_d) with units $m^{-1}\cdot(mg\ DOM\cdot liter^{-1})^{-1}$.

	Y	$A_D'(\lambda_0 = 380)$
Højerslev (Nyquist)	0.014	0.565
Jerlov	0.0147	0.325
Okami et al.	0.01675	0.275
Stuermer Coastal	0.0175	2.160
Stuermer Sargasso	0.020	0.2456

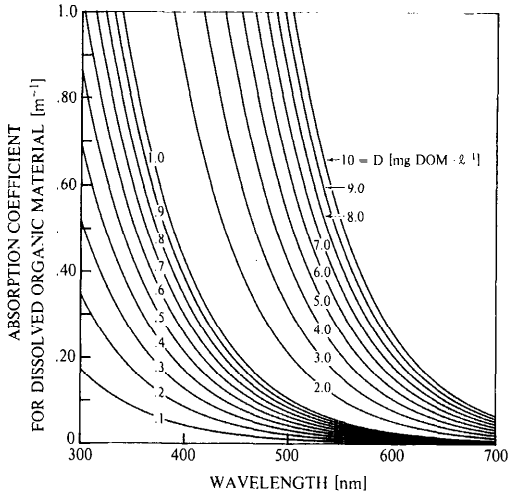

Fig. 6. Absorption coefficient for DOM as determined by Eq. 10 and Højerslev (1980) parameters in Table 4 for a range of D values.

wavelength λ_0. Further, Højerslev (1980), reviewing earlier work on the subject, stated that the postulated (Kalle 1966) direct proportionality between fluorescence and DOM can be found in waters where mixing is pronounced, i.e.

$$A_D(\lambda_0) = A_D'(\lambda_0)\cdot D \qquad (9b)$$

where $A_D'(\lambda_0)$ has units of $m^{-1}\cdot(mg\ DOM\cdot liter^{-1})^{-1}$ and D has units of mg $DOM\cdot liter^{-1}$. In Fig. 5 we present several absorption curves, with their corresponding parameters, as described in Table 4. Although there is general agreement (±14%) with respect to the exponent (Y) parameter (i.e. the curve shapes), there is so far no general agreement with respect to the absolute value of the absorption at a fixed wavelength.

To provide a quantitative DOM component to our classification model we assume that the diffuse attenuation due to DOM, $K_D(\lambda)$, will have a wavelength dependence similar to that of $A_D(\lambda)$. This is equivalent to assuming that the contribution of backscattering to $K_D(\lambda)$ will be relatively independent of wavelength. This assumption needs further investigation but is sufficient for our present requirements. Further, given the uncertainty in the absolute value of $A_D(380)$, we have adopted, for a first approximation of a $K_D(\lambda)$ DOM component, Højerslev's (1980) values:

$$K_D(\lambda) = k_d(\lambda_0)\cdot D\cdot\exp[-k_d'(\lambda - \lambda_0)] \qquad (10)$$

where $\lambda_0 = 380$ (nm), $k_d' = 0.014$ $(0.014\cdot nm^{-1})$, $k_d(\lambda_0) = 0.565$ $[m^{-1}\cdot(mg\ DOM\cdot liter^{-1})^{-1}]$, $D = D$ (mg $DOM\cdot liter^{-1}$), and where the slope value of $0.014\cdot nm^{-1}$ has been validated by Bricaud et al. (1981).

In Fig. 6 a family of curves based on Eq. 10 is presented for a range of DOM concentrations. By fitting the "residual DOM" curves shown in Fig. 4 to Eq. 10, we can get derived values of DOM. We tried to determine DOM in the field experimentally by traditional techniques, but the levels present were so low that no successful measurement was made. The present field techniques have a limit of detection in the range of 0.09 mg $DOM\cdot liter^{-1}$. Since we have no independent measure of actual DOM when our optical data were obtained, this DOM component of our classification model lacks the quantified link to independent measurements that is already incorporated in the chlorophyll component. Indeed, this component of the model is presented as a hypothesis to encourage contemporaneous DOM and optical measurements in various types of ocean water. However this optical determina-

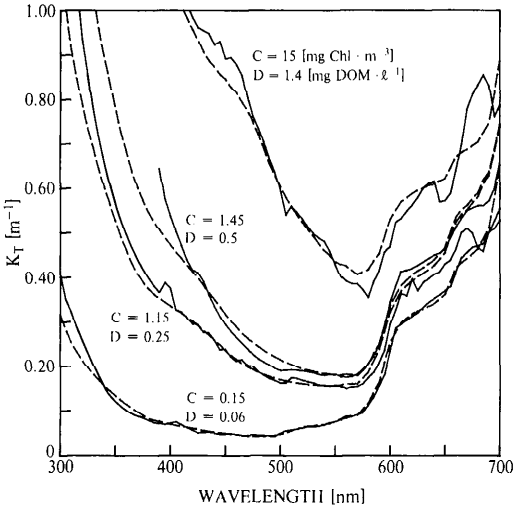

Fig. 7. Spectral diffuse attenuation coefficient vs. wavelength. Solid lines represent optical field measurements for which chlorophyll and dissolved organic material were measured concurrently. Broken lines represent calculated values of $K_T(\lambda)$ using model as described in Tables 2 and 3. Comparison illustrates how model reproduces field data.

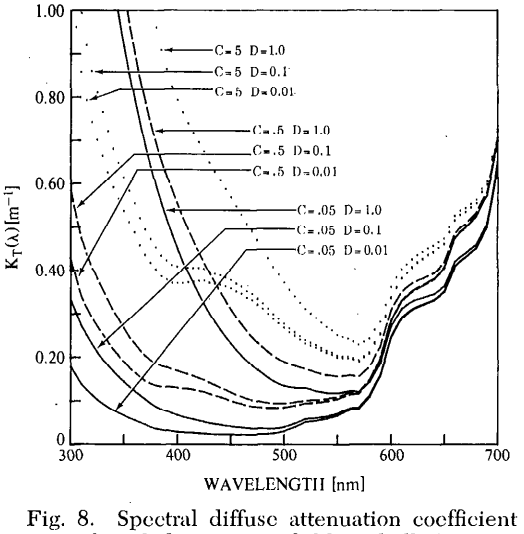

Fig. 8. Spectral diffuse attenuation coefficient vs. wavelength for a range of chlorophylls (mg pigment·m $^{-3}$) and dissolved organic material (mg DOM·liter^{-1}) calculated using model as summarized in Tables 2 and 3.

tion of DOM seems to have the distinct advantage of being many times more sensitive than chemical analytic techniques for the measurement of DOM.

In Fig. 7 experimentally determined $K_T(\lambda)$ data are compared with values of $K_T(\lambda)$ calculated with Eq. 6 and 10, the tabulated parameters in Table 3, the corresponding but independently measured C_K, and the fitted value of D. Agreement between measured and calculated curves is good.

Conclusions

The bio-optical classification model outlined here provides systematic order to a wide range of experimental spectral irradiance data; a continuous index of $K_T(\lambda)$ in terms of the primary biogenous factors influencing the optical properties; an analytic form with which to fit limited $E(z,\lambda)$ data that then allows these data to be extended and used with the facility of mathematical formula; a predictive model for $K_T(\lambda)$ when the principal factors (C_K and DOM) are known or postulated; and the ability to calculate $E(z,\lambda)$ for the study of aquatic photoprocesses.

Equations 6 and 10 comprise a classification scheme for ocean waters whose optical properties are dominated primarily by biogenous material. These equations are summarized in Table 2, and the constant coefficients listed in Table 3. It is clearly a "bio-optical" classification scheme because the input parameters are chlorophyll and dissolved organic material, which allow calculation of the output parameter $K_T(\lambda)$. Whereas the Jerlov classification scheme based on water type has proven useful in describing water types, it is usually difficult to determine quantitatively a water type in the field unless spectral irradiance measurements are made. The model presented here allows a straightforward calculation based on standard biological measurements.

The optical classification model can generally reproduce $K_T(\lambda)$ curves within $\pm 10\%$ over the spectral range from 300 to 700 nm for biogenous waters that vary independently in chlorophyll and DOM concentrations by as much as three orders of magnitude.

The analytic equations of this model

can be used in sensitivity analysis studies of aquatic photoprocesses that require a knowledge of $E(z,\lambda)$. Thus, computations involving photosynthesis, chemical photolysis (Zepp and Aire 1977), and biological dose rates (Smith and Baker 1979) are readily made. Elsewhere (Smith and Baker 1979; Baker and Smith in press) we have shown how $E(0^-,\lambda)$ (a required input to Eq. 1) can be obtained from an atmospheric model (Baker et al. 1980), how $K_T(\lambda)$ is determined from our bio-optical model, and how these results can be used to calculate biologically effective doses (or the energy available for an aquatic photoprocess of interest) as a function of depth in various natural waters.

Further, we emphasize that this is more than a classification scheme. It is also a predictive model for $K_T(\lambda)$. The biological inputs to this model can be varied to produce a variety of ocean water types. This is illustrated in Fig. 8 where $K_T(\lambda)$ values derived from the model by systematically varying C_K and D are shown. All the significant features of the actual $K_T(\lambda)$ data discussed above are present in these calculated curves. A knowledge of $K_T(\lambda)$ then permits calculation of the spectral radiant energy penetrating to depth.

References

BAKER, K. S., AND R. C. SMITH. 1979. Quasi-inherent characteristics of the diffuse attenuation coefficient for irradiance. Ocean Optics 6. Proc. Soc. Photoopt. Inst. Eng. **208:** 60–63.

———, AND ———. In press. Spectral irradiance penetration into natural waters. *In* Solar ultraviolet radiation in marine ecosystems. NATO Adv. Stud. Inst. Proc. Plenum.

———, ———, AND A. E. GREEN. 1980. Middle ultraviolet radiation reaching the ocean surface. Photochem. Photobiol. **32:** 367–374.

BOOTH, C. R. 1976. The design evaluation of a measurement system for photosynthetically active quantum scalar irradiance. Limnol. Oceanogr. **21:** 326–336.

BRICAUD, A., A. MOREL, AND L. PRIEUR. 1981. Absorption by dissolved organic matter of the sea (yellow substance) in the UV and visible domains. Limnol. Oceanogr. **26:** 43–53.

DUNTLEY, S. Q., R. W. AUSTIN, W. H. WILSON, D. F. EDGERTON, AND S. E. MORAN. 1974. Ocean color analysis. Scripps Inst. Oceanogr. Ref. 74-10. 67 p.

GORDON, H. R. 1979. Diffuse reflectance of the ocean: The theory of its augmentation by chlorophyll *a* fluorescence at 685 nm. Appl. Opt. **18:** 1161–1166.

HØJERSLEV, N. K. 1974. Daylight measurements for photosynthetic studies in the western Mediterranean. Univ. Copenhagen Inst. Phys. Oceanogr. Rep. 26. 38 p.

———. 1980. On the origin of yellow substance in the marine environment. Univ. Copenhagen Inst. Phys. Oceanogr. Rep. 42. 35 p.

JERLOV, N. G. 1951. Optical studies of ocean waters. Rep. Swed. Deep-Sea Exped. **3:** 1–59.

———. 1976. Marine optics. Elsevier.

———, AND K. NYGÅRD. 1969. A quanta and energy meter for photosynthetic studies. Univ. Copenhagen Inst. Phys. Oceanogr. Rep. 10. 29 p.

KALLE, K. 1966. The problem of gelbstoff in the sea. Oceanogr. Mar. Biol. Annu. Rev. **4:** 91–104.

KIEFER, D. A., R. J. OLSON, AND W. H. WILSON. 1979. Reflectance spectroscopy of marine phytoplankton. Part 1. Optical properties as related to age and growth rate. Limnol. Oceanogr. **24:** 664–672.

KIRK, J. T. 1976. Yellow substance (Gelbstoff) and its contribution to the attenuation of photosynthetically active radiation in some inland and coastal south-eastern Australian waters. Aust. J. Mar. Freshwater Res. **27:** 61–71.

MOREL, A., AND L. PRIEUR. 1975. Analyse spectrale des coeffients d'atténuation diffuse, d'absorption et de rétrodiffusion pour diverses régions marines. C. R. Oceanogr. Villefranche-sur-Mer Rapp. 17. 157 p.

———, AND ———. 1977. Analysis of variations in ocean color. Limnol. Oceanogr. **22:** 709–722.

———, AND R. C. SMITH. 1974. Relation between total quanta and total energy for aquatic photosynthesis. Limnol. Oceanogr. **19:** 591–600.

NYQUIST, G. 1979. Investigation of some optical properties of sea water with special reference to lignin sulfonates and humic substances. Ph.D. thesis, Univ. Goteborg. 200 p.

OKAMI, N., M. KISHINO, S. SUGIHARA, N. TAKEMATSU, AND S. UNOKI. In press. Analysis of ocean color spectra (3); Measurements of optical properties of sea water. J. Oceanogr. Soc. Jap.

PREISENDORFER, R. W. 1976. Hydrological optics. NOAA.

———. 1979. Empirical determinations of the local and global optical properties of irradiance fields in the sea. Ocean Optics 6. Proc. Soc. Photoopt. Inst. Eng. **208:** 56–59.

RILEY, G. A. 1956. Oceanography of Long Island Sound, 1952–1956. Bull. Bingham Oceanogr. Collect. **15:** 15–46.

SHIBATA, K. 1958. Spectrophotometry in intact biological materials. J. Biochem. Tokyo **45:** 599–604.

SMITH, R. C. 1973. Spectral and total irradiance data. Data Rep. SCOR *Discoverer* Expedition. Scripps Inst. Oceanogr. Ref. 73-16. 160 p.

———, AND K. S. BAKER. 1978*a*. The bio-optical state of ocean waters and remote sensing. Limnol. Oceangr. **23:** 247–259.

———, AND ———. 1978*b*. Optical classification of natural waters. Limnol. Oceanogr. **23:** 260–267.

———, AND ———. 1979. Penetration of UV-B and biologically effective dose-rates in natural waters. Photochem. Photobiol. **29:** 311–323.

———, AND ———. 1981. Optical properties of the clearest natural waters (200–800 nm). Appl. Opt. **20:** 177–184.

———, ———, AND P. DUSTAN. 1981. Fluorometer techniques for the measurement of oceanic chlorophyll in the support of remote sensing at the visibility laboratory. Scripps Inst. Oceanogr. Ref. 81-17.

———, R. L. ENSMINGER, R. W. AUSTIN, J. D. BAILEY, AND G. D. EDWARDS. 1979. Ultraviolet submersible spectroradiometer. Ocean Optics 6. Proc. Soc. Photoopt. Inst. Eng. **208:** 27–140.

———, AND J. E. TYLER. 1968. Spectral irradiance data. Scripps Inst. Oceanogr. Ref. 68-29. 30 p.

STEELE, J. H., AND D. W. MENZEL. 1962. Conditions for maximum primary production in the mixed layer. Deep-Sea Res. **9:** 39–49.

STRICKLAND, J. D., AND T. R. PARSONS. 1968. A practical handbook of seawater analysis. Bull. Fish. Res. Bd. Can. 167.

STUERMER, D. H. 1975. The characterization of humic substances in sea water. Ph.D. thesis, Mass. Inst. Technol.–Woods Hole Oceanogr. Inst. 163 p.

TAKEMATSU, N., M. KISHINO, AND N. OKAMI. 1979. Optical properties and modeling of turbidity components in sea water. Bull. Soc. Fr.-Jap. Oceanogr. **17:** 9–18.

TYLER, J. E. 1975. The in situ quantum efficiency of natural phytoplankton populations. Limnol. Oceanogr. **20:** 976–980.

———, AND R. C. SMITH. 1966. Submersible spectroradiometer. J. Opt. Soc. Am. **56:** 1390–1396.

———, AND ———. 1967. Spectroradiometric characteristics of natural light underwater. J. Opt. Soc. Am. **57:** 595–601.

———, AND ———. 1970. Measurement of spectral irradiance underwater. Gordon and Breach.

YENTSCH, C. S. 1962. Measurements of visible light absorption by particulate matter in the ocean. Limnol. Oceanogr. **7:** 207–217.

———. 1963. Primary production. Oceanogr. Mar. Biol. Annu. Rev. **1:** 157–175.

———. 1979. Biochemical factors affecting the attenuation of visible light in sea water with reference to phytoplankton photosynthesis. Bigelow Lab. Ocean Sci. Contrib. 78002. 36 p.

———, AND C. A. REICHERT. 1962. The interrelationship between water-soluble yellow substances and chloroplastic pigments in marine algae. Bot. Mar. **3:** 67–74.

ZEPP, R. G., AND D. M. AIRE. 1977. Rates of direct photolysis in aquatic environment. Environ. Sci. Technol. **11:** 359–366.

Submitted: 27 April 1981
Accepted: 21 September 1981